Journal of Cell Science 107, 2875-2886 (1994)
Printed in Great Britain © The Company of Biologists Limited 1994

Molecular genetic truncation analysis of filament assembly and phosphorylation domains of *Dictyostelium* myosin heavy chain

Randall J. Lee[1,*], Thomas T. Egelhoff[2] and James A. Spudich

Departments of Biochemistry and Developmental Biology, Stanford University School of Medicine, Stanford, CA, USA

[1]Present address: Department of Medicine and Cardiovascular Research Institute, University of California at San Francisco, San Francisco, CA 94134-1354, USA
[2]Present address: Department of Physiology and Biophysics, Case Western Reserve School of Medicine, Cleveland, OH 44106-4970, USA
*Author for correspondence

SUMMARY

Conventional myosin ('myosin II') is a major component of the cytoskeleton in a wide variety of eukaryotic cells, ranging from lower amoebae to mammalian fibroblasts and neutrophils. Gene targeting technologies available in the *Dictyostelium discoideum* system have provided the first genetic proof that this molecular motor protein is essential for normal cytokinesis, capping of cell surface receptors, normal chemotactic cell locomotion and morphogenetic shape changes during development. Although the roles of myosin in a variety of cell functions are becoming clear, the mechanisms that regulate myosin assembly into functional bipolar filaments within cells are poorly understood. *Dictyostelium* is currently the only system where mutant forms of myosin can be engineered in vitro, then expressed in their native context in cells that are devoid of the wild-type isoform. We have utilized this technology in combination with nested truncation and deletion analysis to map domains of the myosin tail necessary for in vivo and in vitro filament assembly, and for normal myosin heavy chain (MHC) phosphorylation. This analysis defines a region of 35 amino acids within the tail that is critical for filament formation both for purified myosin molecules and for myosin within the in vivo setting. Phosphorylation analysis of these mutants in intact cytoskeletons demonstrates that the carboxy-terminal tip of the myosin heavy chain is required for complete phosphorylation of the myosin tail.

Key words: *Dictyostelium*, myosin, assembly, phosphorylation

INTRODUCTION

In both muscle and nonmuscle cells, conventional myosin assembles into bipolar filaments forming the active unit involved in force production in vivo. In muscle cells, 'thick' filaments are relatively stable structures that assemble to distinct sizes characteristic of organism and muscle cell type. In nonmuscle cells, myosin filaments appear to be dynamic structures that undergo assembly, disassembly and directed translocation (Kolega and Taylor, 1993; Yumura et al., 1984; Berlot et al., 1985, 1987). Although it is known that sequences within the α-helical coiled-coil tail domain of myosin are responsible for driving formation of the bipolar filaments, analysis of assembly domains has only been performed in vitro in most systems, using proteolytic or recombinant tail fragments (De Lozanne et al., 1987; O'Halloran et al., 1990; Sinard et al., 1990; Atkinson and Stewart, 1992). Determining the molecular mechanism by which cells regulate filament assembly requires an understanding of the determinants that drive filament assembly within cells, as well as an understanding of the signaling mechanisms that modulate assembly.

Phosphorylation has been implicated as playing regulatory roles in myosin function in a variety of systems (reviewed by Tan et al., 1992), but the exact role of light chain and heavy chain phosphorylation in modulating filament assembly in vivo is not currently resolved. In smooth muscle myosin, it has been demonstrated that light chain phosphorylation is necessary for efficient filament formation in vitro (Trybus, 1991), and it is generally believed that this holds true within smooth muscle cells as well. However, it has also been suggested that heavy chain phosphorylation may play a role in filament assembly for smooth muscle myosin (reviewed by Kelley et al., 1991; Somlyo, 1993). The intractability of smooth muscle cells to molecular genetic manipulation, however, has generally precluded in vivo tests of either possibility. In mammalian nonmuscle systems, both light chain and heavy chain phosphorylation have been observed during cytoskeletal contractile events (Kolodney and Elson, 1993; Ludowyke et al., 1989; Sagara et al., 1983), and again in vivo tests for the relative roles of heavy and light chain phosphorylation in regulating filament assembly have been difficult to establish.

In *Dictyostelium* substantial evidence now exists to show that myosin heavy chain (MHC) phosphorylation regulates filament assembly (and localization) within cells. MHC can be phosphorylated on threonine residues in the tail, and this inhibits filament formation in vitro (Pagh et al., 1984; Coté and McCrea, 1987; Ravid and Spudich, 1989). Mutation of three

mapped target sites for a 130 kDa MHCK, at residues 1823, 1833 and 2029 (Vaillancourt et al., 1988; Luck-Vielmetter et al., 1990), to alanine renders cells unable to regulate myosin localization in vivo (Egelhoff et al., 1993). These targets lie in a region of the tail close to but not overlapping a region that appears to be involved in driving filament formation. In a detailed proteolytic analysis, Pagh et al. (1984) initially demonstrated that two phosphorylation sites situated approximately 32-38 kDa from the carboxyl end of the tail lay adjacent to a central chymotryptic fragment of 85 kDa, which appeared important for assembly. Analysis conducted with recombinant tail fragments further demonstrated that a discrete tail fragment of 34 kDa was sufficient for in vitro assembly (O'Halloran et al., 1990). Isolated tail fragments studied by these methods, however, do not form true bipolar myosin filaments, but rather form paracrystalline arrays.

We have used parallel analysis of in vitro myosin assembly and in vivo myosin function to further define sequences involved in filament assembly, and to confirm that sequences involved in paracrystal formation in vitro correlate with sequences important for bipolar filament formation and myosin function in vivo. Our analysis has identified a 35 amino acid region essential for filament assembly that lies immediately adjacent to two threonine phosphorylation sites. This result provides support for a previously proposed model (Luck-Vielmetter et al., 1990) that the region of the tail surrounding the 1823 and 1833 threonine phosphorylation sites may play a critical role in filament assembly.

MATERIALS AND METHODS

Strategy for truncations

The design of the sequential carboxyl-terminal myosin tail truncations was based upon three considerations: conservation of the 28 amino acid periodicity found in the *Dictyostelium* tail sequence (Warrick and Spudich, 1987); the threonine phosphorylation sites, residues 1823, 1833 and 2029 (Luck-Vielmetter et al., 1990); and the in vitro studies of assembly that have defined a 34 kDa fragment in the tail (N-LMM-34) as necessary for assembly (O'Halloran et al., 1990). The sequential truncated myosins are shown in Fig. 1, below. Truncation 1 (T1) is a 15.4 kDa truncation of the carboxyl terminus. This fragment eliminates the threonine phosphorylation site 2029, but maintains the majority of the myosin tail between threonine residue 1833 and threonine residue 2029. Truncation 2 (T2) is a 27.6 kDa truncation of the carboxyl terminus of the myosin tail. It eliminates the threonine phosphorylation site 2029 but preserves the two remaining threonine phosphorylation sites. This fragment also contains N-LMM-34, which has been shown to be necessary for assembly of tail fragments expressed in *Escherichia coli* (O'Halloran et al., 1990). Truncation 3 (T3) is a 36.5 kDa truncation of the carboxyl terminus of the myosin tail. It eliminates all the threonine phosphorylation sites and the carboxyl portion of N-LMM-34. Truncation 4 (T4) is a 49.4 kDa truncation of the carboxyl terminus of the myosin tail. It eliminates all the threonine phosphorylation sites and approximately half of N-LMM-34.

Plasmid constructs

Standard methods were used for all DNA manipulations (Sambrook et al., 1989). The vector backbone for all initial constructs was the plasmid pDE109 (Egelhoff et al., 1989), which contains the hygromycin resistance transformation marker and the Ddp2 sequence conferring replication on *Dictyostelium*. A plasmid containing the myosin gene with truncation 4 (T4) was constructed first as follows. Two oligonucleotides were synthesized to introduce sequence modifications via PCR. The first of these, TEROD 1 (5′-GATAAATCTG-GTACCGTC-3′), spans the *Kpn*I site of the myosin heavy chain tail at position 4581 and corresponds to the sense strand of the myosin heavy chain gene. The second oligonucleotide, TEROD 2 (5′-CGTTGATCACGCG**TTA**GCATTGAGAGCAGCACG-3′), corresponds to the antisense strand of the myosin heavy chain gene. The 3′ end of the myosin fragment was engineered to include a stop codon (shown in bold on the antisense strand above), a unique *Mlu*I restriction site and a *Bcl*I restriction site. The stop codon occurs after nucleotide 5004 of the myosin coding region, making the alanine 1668 of the polypeptide the terminal amino acid of the T4 protein. The wild-type myosin heavy chain gene was used as a template for PCR with the TEROD 1 and TEROD 2 primers. The resulting PCR product was cloned into pTZ18 and its sequence was confirmed. To ensure reliable transcription termination, a 265 bp fragment of the 3′ flanking sequence from the wild-type myosin gene (from the *Hin*dIII site at 6345 to the *Bgl*II site at 6610) was cloned directly downstream of the PCR product, and downstream of this myosin terminator region a 0.7 kb 3′ flanking fragment of the *Dictyostelium* actin 15 gene was also introduced. This actin gene fragment corresponds to the terminator region of the plasmid pA15TX (Cohen et al., 1986). This entire cartridge was then isolated with *Kpn*I (which restricts at the upstream end of the PCR-derived product) and with *Spe*I (which restricts within the actin 15 terminator fragment). The purified cartridge was then inserted into the vector pSB2 (Egelhoff et al., 1991). pSB2 contains the entire myosin gene cloned into vector pDE109. In pSB2 expression of the myosin gene is driven by an actin 15 promoter and terminated by an actin 15 terminator fragment. pSB2 was restricted with *Kpn*I and *Spe*I. This digest removes the wild-type myosin tail fragment from pSB2. The isolated truncated tail fragment cartridge was inserted into the restricted pSB2. This plasmid was named pDE122 and expresses the T4 truncated myosin described in this paper.

The series of myosin genes with shorter truncations (T1, T2 and T3) were produced by PCR, cloned into PTZ18, the sequence was then confirmed and exchanged with the *Kpn*I-*Mlu*I fragment of pDE122. Each of these three truncated fragments used TEROD 1 as the upstream sense strand primer. The downstream antisense strand primers used to construct each truncation are described below. Each of these oligonucleotides contains an introduced stop codon (shown in bold) and a *Mlu*I restriction site downstream of the stop codon. Truncation T1 was made utilizing the downstream olionucleotide (5′-CGTGGATCCACGCG**TTA**GTTGGTACGAGCGATGGA-3′), which makes the asparagine at position 1976 the terminal amino acid. Truncation T2 was made with oligonucleotide (5′-CGTGGATC-CACGCG**TTA**GGCTTGAGTGGCTTTGGC-3′), which makes the alanine at position 1865 the terminal amino acid. Truncation T3 was made with oligonucleotide (5′-CGTGGATCCACGCG**TTA**G-GCACGTTCAGATTCGTTC-3′), which makes the alanine at position 1784 the terminal amino acid. The final T1, T2 and T3 truncated myosin constructs in the pDE109 backbone were named pDE127, pDE123 and pDE129, respectively.

All in vivo studies initially used truncated myosins expressed using the pDE109-based plasmids. However, plasmid instability with the pDE109 constructs expressing T3 and T4 was noted. Therefore, all truncations were recloned into the pBIG expression vector (B. Patterson, unpublished data) to correct for plasmid instability. The in vivo studies were repeated using pBIG and the phenotypes observed were similar to those observed using the pDE109-based expression system.

pBIG is derived from pATANB43 (Dynes and Firtel, 1989). This vector contains the native *Dictyostelium* extrachromosomal plasmid Ddp1, which confers autonomous replication on *Dictyostelium*, and the actin 6 promoter-neomycin resistance gene cartridge, which permits growth in the presence of the antibiotic G418. The *Ddp*I sequences and the neomycin cartridge were recloned into *Escherichia*

coli vector pBlueScript II SK (Stratagene) to create pBIG (Patterson et al., unpublished data). The *Dictyostelium* myosin heavy chain (MHC) coding region was derived from the plasmid pMyDAP (Egelhoff et al., 1990) and inserted into pBIG, which was restricted with *Bam*HI and *Sac*I. This version of the MHC gene (pBIG-WT) has the *Dictyostelium* actin 15 promoter fused to the 5′ end of the myosin coding region. T1, T2, T3 and T4 were cloned into the pBIG vector by restricting pDE127 (T1), pDE123 (T2), pDE129 (T3) and pDE122 (T4) with *Sac*I and *Bam*HI, purifying these fragments and inserting them into pBIG-WT, which had been restricted with *Sac*I and *Bam*HI.

Dictyostelium cell line and expression

The myosin null cell line HS1 was constructed from the $MHC^{+}THY^{-}$ cell line JH010 (kindly provided by R. Firtel) as described by Ruppel et al. (unpublished data). Briefly, the plasmid pDMHC-A5 (Manstein et al., 1989) contains a G418 resistance gene cartridge positioned between 5′ and 3′ flanking DNA sequence segments from the *Dictyostelium* MHC gene. The G418 resistance cartridge was removed from this plasmid and replaced with an endogenous *Dictyostelium* gene, THY1 (Dynes and Firtel, 1989), which confers thymidine prototrophy on JH010 cells. This construct was used to disrupt the MHC locus in JH010 cells using the approach described by Manstein et al. (1989).

Expression of the wild-type and mutant myosin heavy chain genes was analyzed by subjecting total protein extracts from 5×10^6 cells to SDS-polyacrylamide gel electrophoresis (SDS-PAGE), followed by Coomassie staining and western blot analysis. Coomassie-stained gels were subjected to densitometric scanning to quantify the expression levels in the different cell lines. Expression levels were quantified as a percentage of wild-type myosin corrected for differences in molecular mass.

Protein purification

The purification protocol for the wild-type, T1 and T2 myosins was adapted from Clarke and Spudich (1974). Cells were grown in 6 liter Erlenmeyer flasks on a gyratory shaker at 200 rpm at 22°C. Each of the myosins was typically purified, starting with 7.5-9.0 liters of culture medium, yielding 40-60 g of cells. Cells were harvested at a density of 5×10^6 cells/ml for 10 minutes at 2500 rpm. The harvested cells were washed once in 1 liter of cold 10 mM Tris-HCl (pH 7.5) and 1 mM EDTA. The cell pellet was resuspended in two volumes/original cell pellet (g) of 10 mM Tris-HCl (pH 7.5), 2 mM EDTA, 1 mM dithiothreitol (DTT) and 40 mM sodium pyrophosphate; and an equal volume (e.g. three volumes/original cell pellet (g)) of 10 mM Tris-HCl (pH 7.5), 2 mM EDTA, 1 mM DTT, 40 mM sodium pyrophosphate, 60% sucrose, 1 mM PMSF, 0.2 mM TPCK (*N*-tosyl-L-phenylalanine chloromethyl ketone) and 0.2 mM TLCK (*N*α-*p*-tosyl-L-lysine chloromethyl ketone) was added. Cells were lysed by sonication with a Heat-System Ultrasonic model W 200-F sonicator equipped with a 0.75 inch tip. Sonication was applied until 90% of the cells were lysed. The cell lysate was adjusted to 0.1 M KCl using a stock 3 M KCl solution and centrifuged at 27,200 ***g*** for 15 minutes. The supernatant was recovered and further centrifuged at 435,680 ***g*** for 90 minutes. An actomyosin pellet was formed by dialyzing the cell lysate supernatant overnight in 10 mM PIPES (pH 6.8), 0.5 mM DTT, 2 mM EDTA, 50 mM KCl, 0.5 mM PMSF and 0.02% sodium azide (dialysis buffer). The actomyosin precipitate was collected by centrifugation at 15,000 rpm for 30 minutes. Extraction of myosin from this pellet was achieved by resuspending the actomyosin pellet in 25 ml of 10 mM HEPES (pH 7.5), 50 mM KCl and 2 mM EDTA (HKE buffer) and homogenizing after the addition of an equal volume of 10 mM HEPES (pH 7.5), 2 mM EDTA, 1 mM DTT, 1.2 M KI, 10 mM ATP and 10 mM $MgCl_2$ (extraction buffer). The resulting extraction solution was clarified at 435,680 ***g*** for 30 minutes. The supernatant was dialyzed overnight in dialysis buffer. The precipitate was collected by centrifugation at 27,200 ***g*** for 15 minutes. Myosin was extracted from this pellet by homogenizing the actomyosin pellet in 2 ml of HKE buffer and an equal amount of extraction buffer in a Dounce-type homogenizer. The myosin suspension was clarified by centrifugation at 75,000 rpm for 30 minutes in a Beckman TL 100.3 rotor. The clarified supernatant was immediately loaded on a gel filtration column that had been equilibrated with 10 mM TES (pH 7.5), 20 mM sodium pyrophosphate, 5% sucrose, 1 mM DTT, 100 mM KCl, 2 mM EDTA and 0.02% sodium azide and preloaded with 50 ml of 10 mM HEPES (pH 7.5), 2 mM EDTA, 1 mM DTT, 0.6 M KCl, 5 mM ATP and 5 mM $MgCl_2$. The myosin fractions, confirmed by Coomassie-stained gels, were pooled and concentrated with Centricon tubes.

Purification of T3 and T4 was performed, based on the method designed for purification of soluble myosin fragments (Uyeda and Spudich, unpublished results). Cells were grown on 24 cm × 24 cm plates, each containing 125 ml of HL5 medium (OXOID, USA). The cells were grown at 22°C in a stationary position until the cells became confluent. The medium was then changed for 250 ml of fresh HL5 medium and the plates were shaken on a gyratory shaker at 60 rpm, at 22°C for 24 hours. Each of the myosins were typically purified from 40 plates, yielding approximately 40 g of cells. The cells, harvested by scraping off the plates with the use of a rubber spatula, were washed as described above. The cell pellet was resuspended in 8 volume/g cells of the cold lysis buffer (25 mM HEPES (pH 8.0), 25 mM NaCl, 10 mM EDTA, 1 mM DTT, 1 mM PMSF, 0.2 mM TPCK and 0.2 mM TLCK). Cells were lysed by sonication as described above. Residual ATP was removed by adding 0.5 mg/ml hexokinase and adjusting the resupension to 10 mM glucose using a stock 1 M glucose solution. The suspension was incubated on ice for 10 minutes. The insoluble fraction was collected by centrifugation at 39,200 ***g*** for 30 minutes. The pellet was washed in 10 volume/g cells in 25 mM HEPES (pH 8.0), 200 mM NaCl, 1 mM EDTA, 1 mM DTT, 1 mM PMSF, 0.2 mM TLCK and 0.2 mM TPCK. The pellet was collected by centrifugation at 39,200 ***g*** for 30 minutes. Extraction of the myosin was achieved by resuspending the pellet in 5 volume/g cells of 10 mM HEPES (pH 8.0), 150 mM NaCl, 4 mM $MgCl_2$, 2 mM ATP, 1 mM DTT, 1 mM PMSF, 0.2 mM TLCK and 0.2 mM TPCK. The solution was centrifuged at 18,000 rpm for 30 minutes and the supernatant was collected. After the addition of 50 μg/ml of RNase A, the supernatant was concentrated to 4 ml by dialyzing the solution against an Aquacide (Calbiochem) solution in 10 mM HEPES (pH 7.5), 25 mM NaCl, 4 mM $MgCl_2$ and 1 mM DTT (Buffer H). The concentrated dialyzate was adjusted to 2 mM ATP using a stock 0.1 M ATP solution and immediately centrifuged at 75,000 rpm for 20 minutes in a Beckman TL 100 ultracentrifuge. The clarified supernatant was immediately loaded on a gel filtration column that had been equilibrated with buffer H and preloaded with 10 mM HEPES (pH 7.5), 0.6 M KCl, 5 mM ATP, 5 mM $MgCl_2$ and 1 mM DTT. The myosin fractions were pooled and concentrated with Centricon tubes.

Electrophoresis methods

Electrophoresis on SDS-polyacrylamide gels (SDS-PAGE) and western blot analysis were performed as described previously (Egelhoff et al., 1991). Western blot detection was performed using the monoclonal anti-*Dictyostelium* myosin antibody My2 (Peltz et al., 1985) and developed using a horseradish peroxidase-coupled secondary antibody (Bio-Rad Laboratories, Richmond CA). Epitope mapping and localization of the assembly domain of the truncated myosins were performed with the anti-*Dictyostelium* myosin antibodies My2, My4 and My5, which were initially localized topographically in the region of the truncations (Flicker et al., 1985).

In vitro filament assembly assay

Filament assembly was performed using a previously described sedimentation assay (Kuczmarski and Spudich, 1980). The purified myosin solutions were dialyzed for 12 hours at 4°C in 5 mM HEPES (pH 7.5), 1 mM EDTA and 1 mM DTT. Following the dialysis, the purified proteins were centrifuged at 131,792 ***g*** for 10 minutes at 4°C

to remove any insoluble or aggregated material. The clarified myosins were then mixed with equal volumes of KCl solutions to yield final KCl concentrations ranging from 0 to 200 mM KCl. After incubation on ice for 15 minutes, the samples were centrifuged at 55,000 rpm for 10 minutes in a Beckman TL 100.3 rotor. Equivalent amounts of supernatant and pellet fractions were subjected to SDS-PAGE. The myosin bands were identified by Coomassie staining and their relative amounts were determined by scanning densitometry.

Growth and development

Growth and development of *Dictyostelium* cells were performed as previously described (Sussman, 1987). Plasmids were introduced into *Dictyostelium* cells using standard electroporation conditions, as described previously (Egelhoff et al., 1991). Electroporated cells were plated in HL5 medium non-selectively overnight and then subjected to antibiotic selection (6 μg/ml for G418 and 18 μg/ml for hygromycin). Colonies typically appeared after 6-8 days. These colonies were transferred to independent Petri dishes by sucking them into a pipetteman tip while scraping gently with the tip. Once confluence was obtained, cells were collected, diluted with HL5 medium to a density of 5×10^4 cell/ml and agitated on a platform at 20-21°C. Determination of growth in suspension of the wild-type and mutant myosin heavy chain gene cells were performed by counting cells at 12, 24, 48, 72 and 96 hours. At least three independent colonies derived from separate platings of the initial electroporation mix were analyzed for each construct. All of the phenotypes observed were reproducible between different isolates.

Capping and immunomicroscopy

Capping and indirect immunofluorescence staining were performed using conditions previously described (Egelhoff et al., 1991). In brief, cells in HL5 medium were allowed to attach to glass coverslips and were then gently rinsed into starvation buffer (20 mM MES (pH 6.8) 2 mM $MgCl_2$, 0.2 mM $CaCl_2$). Tetramethylrhodamine-conjugated concanavalin A (Con A, 40 μg/ml; Sigma) in starvation buffer was applied for 1 minute, followed by a rinse back to plain starvation buffer. A small agar sheet was then gently laid onto the pool of buffer lying over the cells (Fukui et al., 1990). Samples were incubated in humid chambers for either 5 minutes or 30 minutes, then fixed in 1% formaldehyde in −10°C acetone for 5 minutes. Following fixation, cells were rinsed in phosphate buffered saline and processed for immunofluorescence using rabbit anti-myosin antiserum for the primary incubation and a fluorescein-conjugated, affinity-purified goat anti-rabbit IgG for the secondary incubation.

Triton-insoluble cytoskeleton analysis

Triton-insoluble cytoskeleton analysis was performed as previously described (Egelhoff et al., 1991). Cells were harvested from HL5 medium, washed once in 50 mM Tris-HCl, pH 7.5, and resuspended in buffer A (0.1 M MES (pH 6.8) 5 mM $MgCl_2$, 2.5 mM EGTA and 0.5 mM ATP) at 3.3×10^6 cells/ml. A 150 μl sample of the cell suspension was then mixed with 150 μl of buffer B (same as buffer A, but also containing 1% Triton X-100, 100 μg/ml PMSF, 50 μg/ml TLCK, 1 μg/ml pepstatin and 1 μg/ml leupeptin) at 0°C. The suspensions were vortexed for 5 seconds and then centrifuged for 1 minute at 4°C in a microcentrifuge. Supernatants were precipitated with 700 μl cold acetone followed by centrifugation. Supernatants and cytoskeletal pellet fractions were then resuspended in SDS-PAGE sample buffer, boiled for 5 minutes and loaded onto 10% polyacrylamide gels. Duplicate gels were run for all samples. One set of samples was stained with Coomassie Blue and the other set was used for western blot analysis. Quantification of the relative amounts of myosin heavy chain in each soluble and cytoskeletal fraction was determined by densitometric scanning.

Myosin phosphorylation and phosphoamino acid analysis

Myosin phosphorylation techniques were adapted from Berlot et al. (1987). Cells expressing WT, T1, T2, T3, T4, ΔC34 (Egelhoff et al., 1990) and MyΔ934-1454 (Kubalek et al., 1993) myosins were harvested from HL5 medium, resuspended in starvation buffer, resuspended at 10^7 cells/ml (500 μl), placed in a 15 ml test tube on a rotating wheel to provide aeration and incubated for 4 hours. A 150 μl sample of the starved-cell suspension was mixed with an equal volume of Triton buffer (0.4% Triton X-100, 5 mM $MgCl_2$, 10 mM Tris-HCl, pH 7.5, 3 mM EGTA, 50 μg/ml PMSF). A 2 μl sample of a 1 M glucose solution and 50 μl of 5 mg/ml hexokinase (Sigma) solution were immediately added to the sample and vortexed at a medium setting for 5 seconds. The sample was then centrifuged for 1 minute at 4°C in a microcentrifuge to collect the Triton-insoluble cytoskeletal fraction. The pellet was resuspended in 30 μl of labeling mix (10 mM Tris-HCl, pH 7.5, 2 mM $MgCl_2$, 50 mM NaCl) containing 100 μCi of [γ-^{32}P]ATP (10 mCi/ml; 3000 Ci/mmole; Amersham) that had been concentrated in a Speed-Vac. The labeling reaction was allowed to proceed for 5 minutes at 0°C. Each sample was then diluted with 500 μl of immunoprecipitation buffer (IP buffer: 40 mM Tris-HCl, pH 7.5, 0.2% Nonidet-40, 2 mM DTT, 10 mM EDTA, 100 μg/ml RNase A, 50 mM sodium pyrophosphate, 200 mM sodium fluoride, 2 mM ATP, 100 μg/ml PMSF, 50 μg/ml TLCK, and 1 μg/ml each of pepstatin and leupeptin) containing Pansorbin (Calbiochem). This suspension was then incubated on a rotor for 10 minutes at 4°C and centrifuged in a microcentrifuge for 30 seconds. An anti-myosin IgG-Pansorbin complex (described below) was then added to the supernatant and incubated on a rotor for 30 minutes at 4°C. The Pansorbin complexes were washed with IP buffer three times. Following the washes, the Pansorbin complexes were suspended in SDS-PAGE gel sample buffer and boiled for 5 minutes. Samples were then electrophoresed on 10% polyacrylamide gels and stained with Coomassie Blue. Autoradiography of the stained gels was performed. Quantification of [^{32}P]orthophosphate levels was done using a Phosphor Imager (Molecular Dynamics). The MHC bands were excised and eluted for phosphoaminoacid (PPA) analysis as described by Boyle et al. (1991). Acid hydrolysis was performed at 110°C for 4 hours to optimize for recovery of phosphothreonine (Cooper et. al., 1983). Anti-myosin IgG was purified from a rabbit anti-myosin antiserum and allowed to complex with Pansorbin as described previously (Berlot et al., 1985). The anti-myosin Pansorbin complex was then suspended in the IP buffer for addition to the phosphorylation reactions.

RESULTS

Expression of truncated MHC gene constructs in *Dictyostelium*

Nested deletions of the myosin heavy chain gene were constructed to allow expression in *Dictyostelium* of myosin molecules with progressively larger and larger portions of the carboxyl terminus of the protein removed (Fig. 1). The T1 truncation (at 1976) removes the mapped phosphorylation site at 2029 and approximately 15 kDa of the coiled-coil myosin tail. Truncation T2 (at 1865) removes approximately 28 kDa of the myosin tail, leaving the 1823 and 1833 phosphorylation target sites situated close to the end of the protein. The previously described ΔC34 truncation (at 1819; Egelhoff et al., 1989) removes all three mapped threonine phosphorylation sites and approximately 34 kDa of the tail. The T3 truncation (at 1784) removes an additional 35 amino acids, and the T4 truncation (at 1668) removes approximately 49 kDa of the myosin tail.

Expression levels were quantified using densitometric analysis of Coomassie Blue-stained protein gels (Fig. 2). Expression levels of T1, T2, T3 and T4 myosin relative to wild

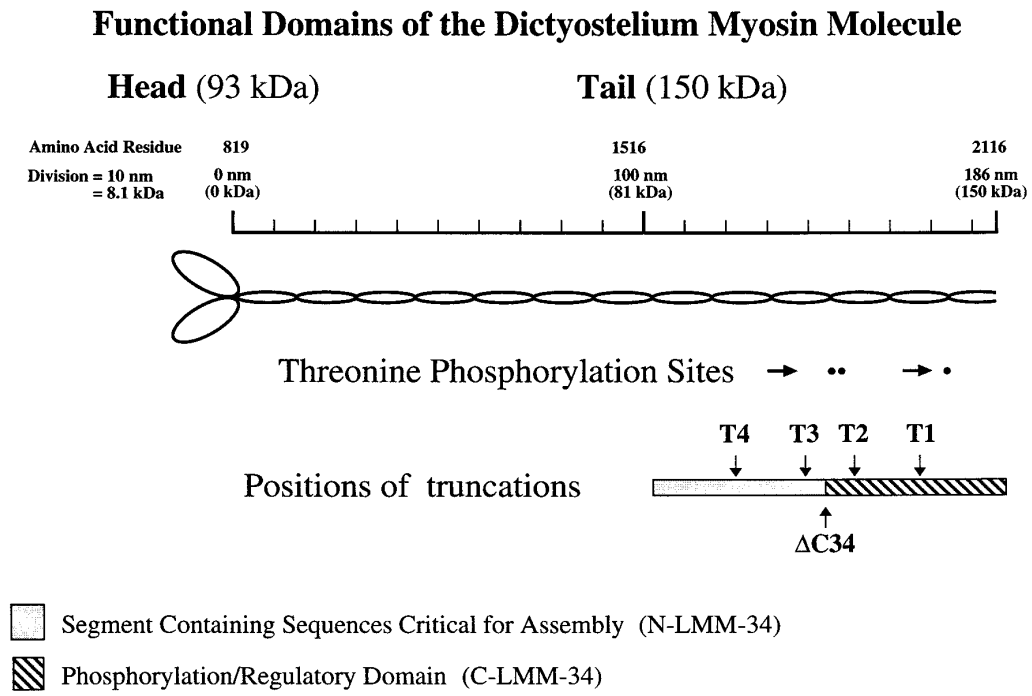

Fig. 1. Schematic representation of *Dictyostelium* myosin illustrating the previously described threonine phosphorylation sites, in vitro assembly domain (N-LMM-34), in vitro phosphorylation regulatory domain (C-LMM-34) and the positions of the myosin truncations for this study. The relative scale of the myosin tail indicates the distance from the head-tail junction; divisions represent 10 nm or 8.1 kDa.

type were 110%, 102%, 50% and 63%. Expression of the ΔC34 myosin has been quantified previously at 42% of wild type (Egelhoff et al., 1989).

Anti-myosin monoclonal antibodies were used to further characterize the truncated myosin molecules. Epitopes for the antibodies My2, My4 and My5 have been mapped and ordered previously within the *Dictyostelium* myosin tail (Peltz et al., 1985; Flicker et al., 1985). Wild-type and truncated myosin whole-cell lysates were subjected to immunoblotting with these monoclonal antibodies. My2 and My5 were able to bind both the wild-type myosin and all of the truncated myosins (Fig. 3A and C). In contrast, My4 was able to bind wild-type, T2 and ΔC34 myosins, but not T3 or T4 myosins (Fig. 3B). These results are consistent with the epitope ordering established by Peltz et al. (1985) and Flicker et al. (1985), and demonstrate that the epitope for the My4 monoclonal antibody lies within the region bounded by the T3 and T4 truncations (1669-1784).

In vitro assembly properties

Truncated myosin molecules were purified from *Dictyostelium* to allow in vitro analysis of assembly properties (Fig. 4). ΔC34 myosin was also subjected to this in vitro assay of assembly. Wild-type, T1, T2 and ΔC34 myosins displayed similar assembly properties, with the greatest solubility at 0 salt and at salt concentrations greater then 150 mM (Fig. 5). A salt concentration in the range of 50-100 mM caused the highest degree of assembly. This corresponds to physiological ionic strength for *Dictyostelium* (Marin and Rothman, 1980), and is also consistent with previously reported solubility data for wild-type non-phosphorylated *Dictyostelium* myosin (Kuczmarski and Spudich, 1980; Cote and McCrea, 1987; Ravid and Spudich, 1989). In contrast, T3 and T4 myosins were predominantly soluble at all salt concentrations, which demonstrates their inability to assemble (Fig. 5). These results demonstrate that truncations beyond residue 1819 (ΔC34 truncation) remove sequences critical for in vitro filament formation.

Growth and development

Assessment of the ability of truncated myosin mutants to undergo cytokinesis properly was performed by placing the full-length and truncated myosin transformants in suspension culture and monitoring growth. The parent myosin null cells were unable to grow in suspension, as previously described for a different myosin null cell line (Manstein et al., 1989). Transformation of the null cells with the wild-type myosin heavy chain gene restored the cells' ability to divide in suspension. T1 and T2 myosin transformants were also able to grow in suspension, indicating their ability to drive cytokinesis. Although T1 myosin cells and T2 myosin cells were able to grow in suspension, they grew at slower rates (doubling times 12-24 hours and 20-30 hours, respectively) than wild-type myosin cells (doubling time 11-14 hours). The morphological appearance of T1 myosin cells was similar to that of the full-length myosin transformant, but the appearance of T2 was abnormal, with a lumpy morphology similar to that of ΔC34 myosin cells observed previously (Egelhoff et al., 1991). T3 and T4 myosin transformants were unable to grow in suspension, suggesting defects in cytokinesis; when placed in suspension culture, they formed large multinucleated cells similar to myosin null cells (Manstein et al., 1989).

Development of the truncated myosin mutants was assessed by their ability to complete the developmental cycle (Sussman, 1987). Myosin-deficient cells can aggregate, but arrest in the loose mound stage (Knecht and Loomis, 1987; De Lozanne and Spudich, 1987; Manstein et al., 1989). Transformation of myosin null cells with the wild-type myosin gene restored the ability of the cells to proceed further and form sorocarps (Fig. 6). Myosin null cells complemented with the T1 MHC gene also aggregated and formed sorocarps at normal rates (Fig. 6).

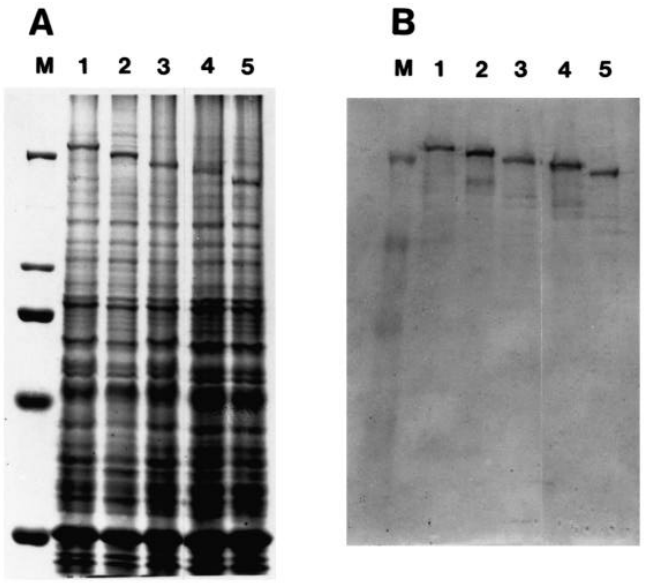

Fig. 2. Expression of myosin cell lines transformed with wild-type and mutated myosin gene constructs. (A) A Coomassie-stained gel of total cell lysates that were subjected to SDS-PAGE.
(B) Corresponding western blot. Lane M, molecular mass standards (from top to bottom: 225 kDa, 94 kDa, 67 kDa, 43 kDa and 30 kDa); lane 1, myosin null cell line transformed with the wild-type myosin gene (pBIG-WT); lane 2, myosin null cell with T1 myosin construct (pBIG-T1); lane 3, myosin null cell with T2 myosin construct (pBIG-T2); lane 4, myosin null cell with T3 myosin construct (pBIG-T3); lane 5, myosin null cell with T4 myosin construct (pBIG-T4).

T2 MHC transformants were able to complete the developmental cycle and form sorocarps. However, the formed sorocarps had shorter stalks and aggregation of cells did not always lead to the formation of sorocarps (Fig. 6). T3 MHC transformants and T4 MHC transformants were arrested in the loose mound stage, an identical terminal morphology as myosin null cells (Fig. 6).

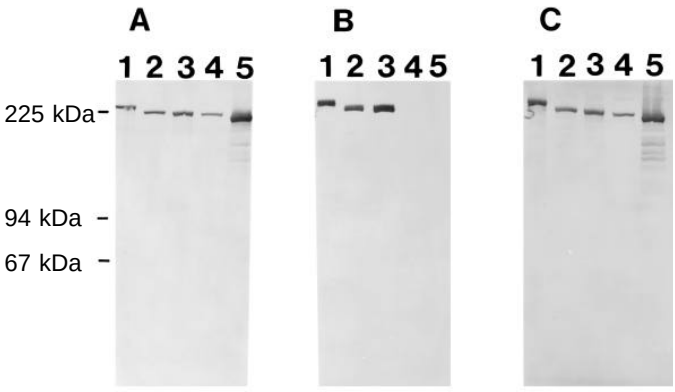

Fig. 3. Epitope mapping of purified recombinant myosin molecules. Monoclonal anti-*Dictyostelium* myosin antibodies, My 2, My 4 and My 5, were used to western blot duplicate samples of purified wild-type myosin, T2 myosin, ΔC34 myosin, T3 myosin and T4 myosin subjected to SDS-PAGE. (A) Western blotting with My 2.
(B) Western blotting with My 4. (C) Western blotting with My 5. Lane 1, wild-type myosin: lane 2, T2 myosin; lane 3, ΔC34 myosin; lane 4, T3 myosin; lane 5, T4 myosin. Molecular mass markers are designated to the left of the figure.

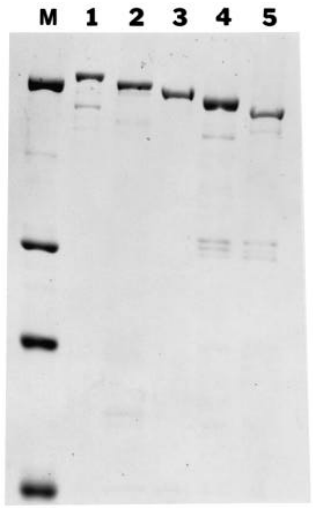

Fig. 4. Purified recombinant myosins. Purified recombinant myosins were subjected to SDS-PAGE and stained with Coomassie Blue. M, molecular mass standards (from top to bottom: 225 kDa, 94 kDa, 67 kDa and 43 kDa); lane 1, wild-type myosin; lane 2, T1 myosin; lane 3, T2 myosin; lane 4, T3 myosin and lane 5, T4 myosin.

Capping of cell surface proteins

Previous reports have shown myosin to be essential for capping of cell surface proteins (Fukui et al., 1990; Pasternak et al.,

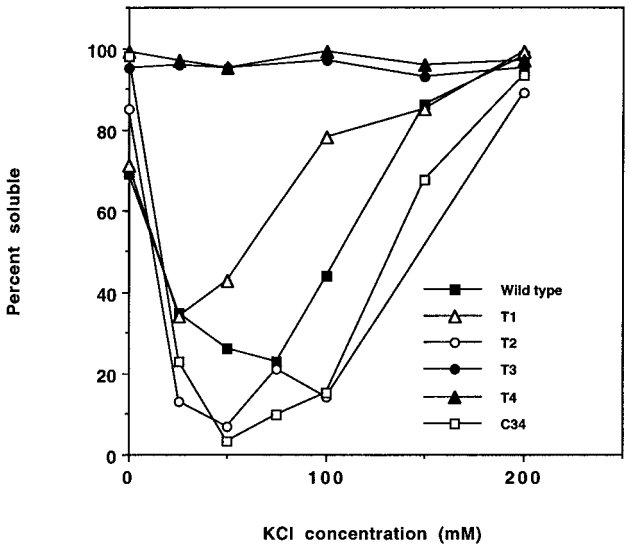

Fig. 5. In vitro assembly of purified recombinant myosin molecules. Purified recombinant myosin molecules were dialyzed into 5 mM HEPES (pH 7.5), 1 mM EDTA and 1 mM DTT, and then mixed with various salt solutions to yields various KCl concentrations. The samples were then centrifuged at 131,792 ***g*** for 15 minutes. Equivalent amounts of supernatants and pellet were subjected to SDS-PAGE and stained with Coomassie Blue. Relative amounts were determined by scanning densitometry. The percentage of each protein remaining in the supernatent (as compared to protein in the pellet) was plotted versus KCl concentrations.

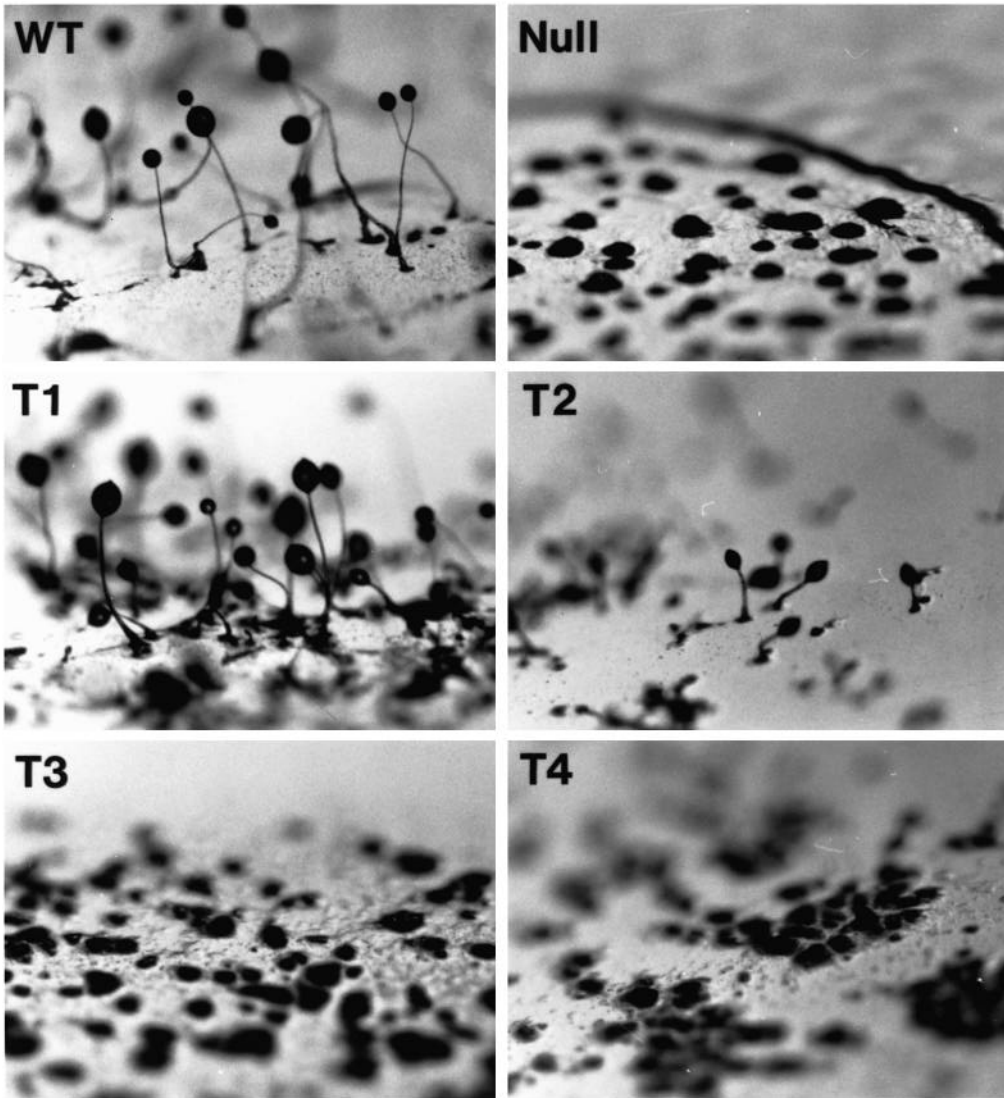

Fig. 6. Development of recombinant cell lines on *Klebsiella aerogenes* lawns. WT, myosin null cells expressing wild-type myosin; Null, myosin null cell line HS1; T1, myosin null cells expressing T1 myosin; T2, myosin null cells expressing T2 myosin; T3, myosin null cells expressing T3 myosin; T4, myosin null cells expressing T4 myosin.

1989). Combining capping of surface receptors with indirect immunofluorescence localization of myosin allows for kinetic assessment of myosin recruitment, localization and disassembly during this in vivo contractile event (Egelhoff et al., 1991). Myosin null cells complemented with the wild-type myosin gene demonstrated a peak of active capping of surface receptors at 5 minutes, associated with myosin enrichment beneath the caps. At 30 minutes following treatment with Con A, these cells displayed a high frequency of completely formed caps, while at this point the myosin has returned to a more homogeneous distribution. The myosin null cells did not demonstrate capping of cell surface proteins at 5 minutes or 30 minutes, or show any myosin immunofluorescent staining. These controls are consistent with earlier observations (Fukui et al., 1990; Pasternak et al., 1989) and similar to the results reported by Egelhoff et al. (1993). Myosin null cells complemented with the T1 MHC gene or the T2 MHC gene demonstrated active capping of surface proteins in response to Con A at both 5 minutes and 30 minutes (Fig. 7A,E and C,G). At 5 minutes, T1 MHC cells and T2 MHC cells were enriched for myosin beneath the caps (B and F), similar to the wild-type cells. However, the myosin enrichment persisted at 30 minutes (D and H). The co-localization of the T1 myosin with the cell surface cap was qualitatively less intense than the co-localization of the T2 myosin with the cell surface cap at 30 minutes following Con A treatment. However, both T1 MHC and T2 MHC cells showed abnormally persistent myosin co-localization at sites of capping relative to that of wild-type cells. T3 and T4 truncated myosin transformants showed no capping response to Con A at either 5 minutes or 30 minutes, and the myosin immunofluorescent staining remained evenly distributed throughout the cytoplasm (Fig. 7I-P).

Myosin localization to cytoskeletal ghosts

Isolation of actin-enriched Triton-insoluble cytoskeleton in the presence of Triton X-100, EGTA and ATP was used to assess the competence of the truncated myosins to assemble into the cytoskeleton. This assay has recently been used to demonstrate over-assembly of another truncated myosin (ΔC34 myosin) that has defective disassembly properties in vivo (Egelhoff et al., 1991). ΔC34 myosin localized predominantly in the Triton-insoluble cytoskeletal fraction. In the present study, myosin in the wild-type MHC transformants localized primarily in the Triton-soluble fraction (Fig. 8, lane 2), while the T1 MHC and

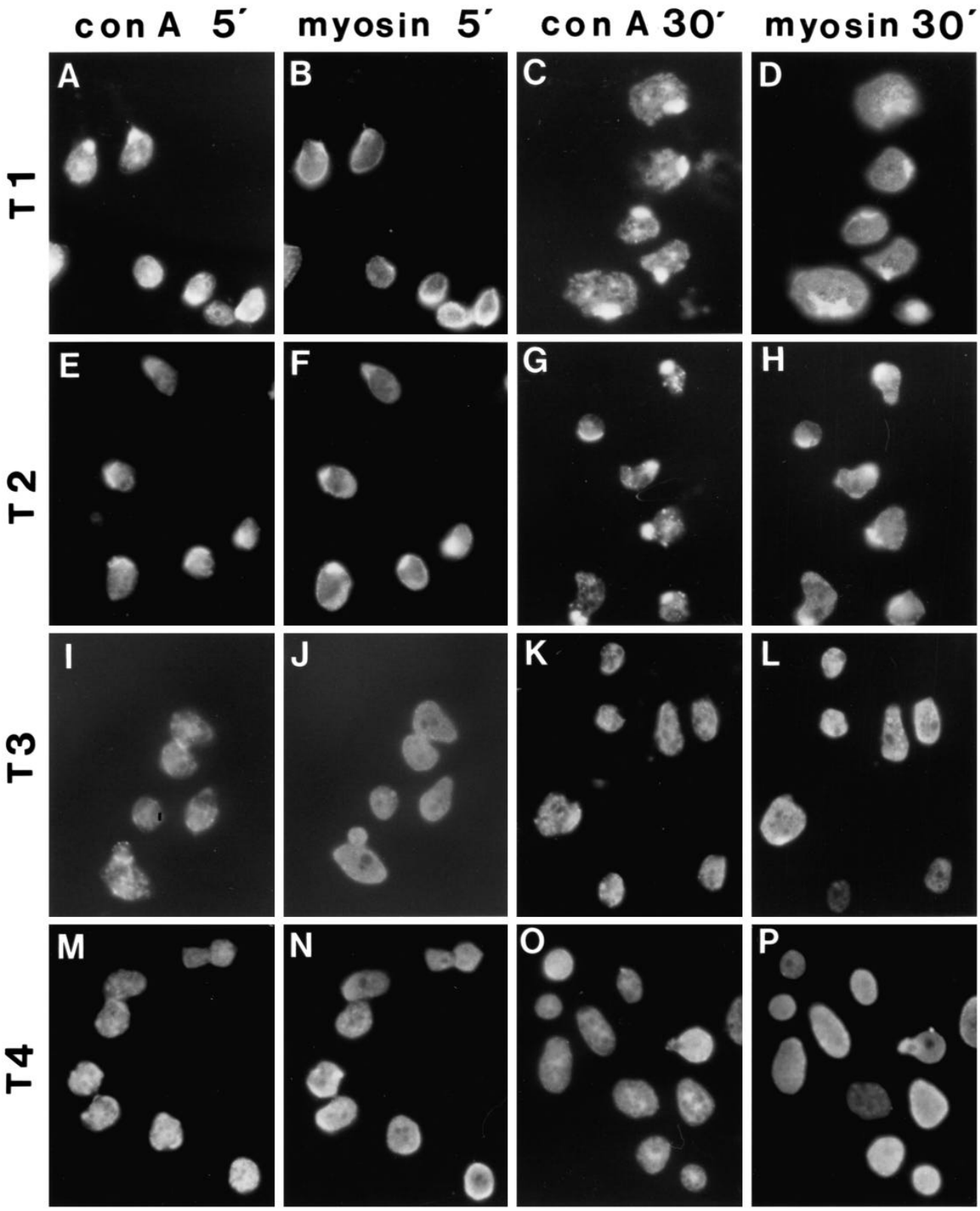

Fig. 7. Capping of cell surface receptors in response to Con A treatment. Cells attached to glass coverslips were treated with Con A, fixed and subjected to indirect immunofluorescence staining at 5 minutes and 30 minutes. The first column demonstrates Con A fluorescence staining in cells fixed at 5 minutes, and the second column demonstrates myosin staining in the same cells. The third column demonstrates Con A fluorescence staining in cells fixed at 30 minutes, and the fourth column demonstrates myosin staining in the same cells. Cell lines are indicated on the left: first row, cells expressing T1; second row, cells expressing T2; third row, cells expressing T3; fourth row, cells expressing T4.

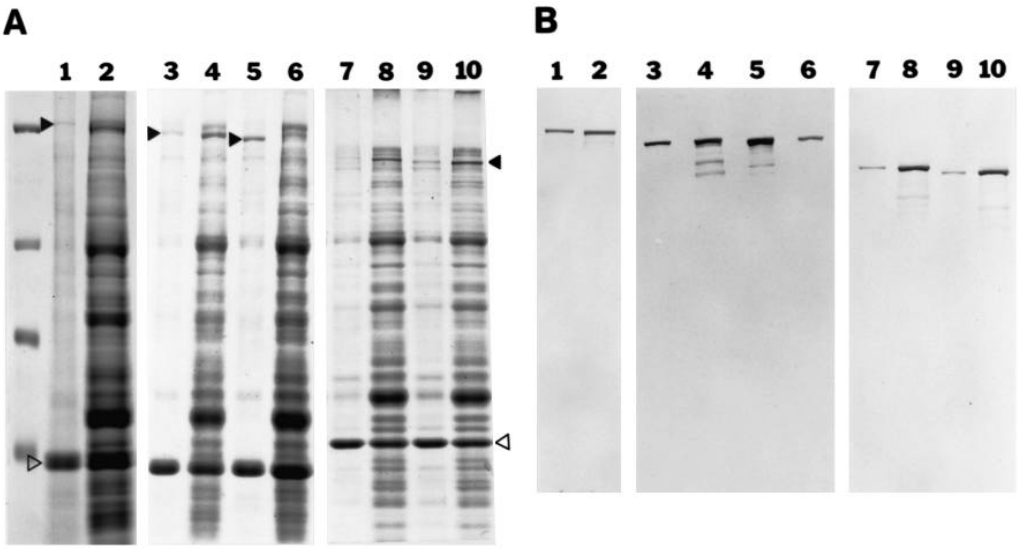

Fig. 8. Recombinant myosin incorporation into Triton X-100-resistant cytoskeletons. Triton-insoluble cytoskeletal fractions and Triton-soluble cytoskeletal fractions of cell lysates were subjected to SDS-PAGE and stained with Coomassie Blue (A). A duplicate gel was subjected to western blotting (B). Filled arrowheads indicate the position of the myosin heavy chain. Open arrowheads indicate the position of actin. Odd numbered lanes represent the Triton-insoluble cytoskeletal fractions while the even numbered lanes represent the Triton-soluble cytoskeletal fractions. Molecular mass standards are located on the left (from top to bottom: 225 kDa, 94 kDa, 67 kDa and 43 kDa). Lanes 1 and 2, cells expressing wild-type myosin; lanes 3 and 4, cells expressing T1; lanes 5 and 6, cells expressing T2; lanes 7 and 8, cells expressing T3; lanes 9 and 10, cells expressing T4.

T2 MHC transformants had considerably more myosin localized in the Triton-insoluble fraction (Fig. 8, lanes 3 and 5). Quantification of the relative amounts of myosin heavy chain in each soluble and cytoskeletal fraction showed that 17% of the full-length myosin, 36% of the T1 myosin and 88% of the T2 myosin was in the Triton-insoluble cytoskeleton. Myosin in T3 MHC and T4 MHC transformants predominantly localized in the Triton-soluble fraction (Fig. 8, lanes 8 and 10). It was estimated that less then 8% of the myosin in T3 MHC and T4 MHC transformants was localized to the Triton-insoluble cytoskeleton.

The over-assembly observed in this assay for T1 and T2 myosin parallels the defective phenotypes of these proteins observed during the capping assay described above.

MHC phosphorylation properties

MHC phosporylation is known to play a key role in regulating myosin localization in *Dictyostelium* (Egelhoff et al., 1993). It has been shown previously that a major threonine-specific MHC kinase co-fractionates with such ghosts (Berlot et al., 1987). Truncated MHC cell lines were tested for competence to phosphorylate MHC in crude cytoskeletal ghosts (Fig. 9). Only T1 and T2 MHC had detectable amounts of phosphorylation. However, quantification of [^{32}P]orthophosphate levels demonstrated that the amount of phosphorylation of the T1 myosin was only 2% of that in the wild-type myosin, while T2 myosin was shown to have less than 1% of that in the wild-type myosin. ΔC34, T3 and T4 myosins did not have any notable phosphorylation (Fig. 9). However, in T2, ΔC34, T3

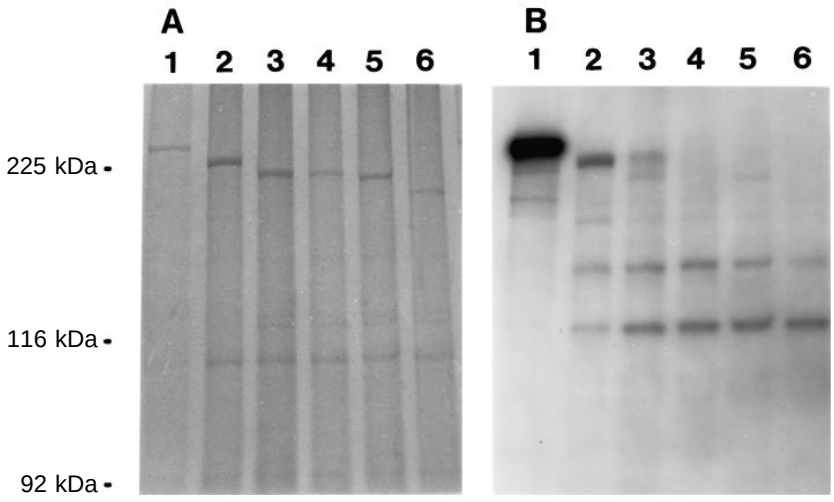

Fig. 9. Phosphorylation of wild-type and truncated myosins in isolated Triton X-100-resistant cytoskeletons. Following phosphorylation of the myosin, it was immunoprecipated, subjected to SDS-PAGE and stained with Coomassie Blue. Autoradiography was performed on the Coomassie-stained gel. (A) Coomassie-stained gel of the immunoprecipitate. (B) Autoradiogram of the Coomassie-stained gel in A. Lane 1, wild-type myosin; lane 2, T1 myosin; lane 3, T2 myosin; lane 4, ΔC34 myosin; lane 5, T3 myosin; lane 6, T4 myosin.

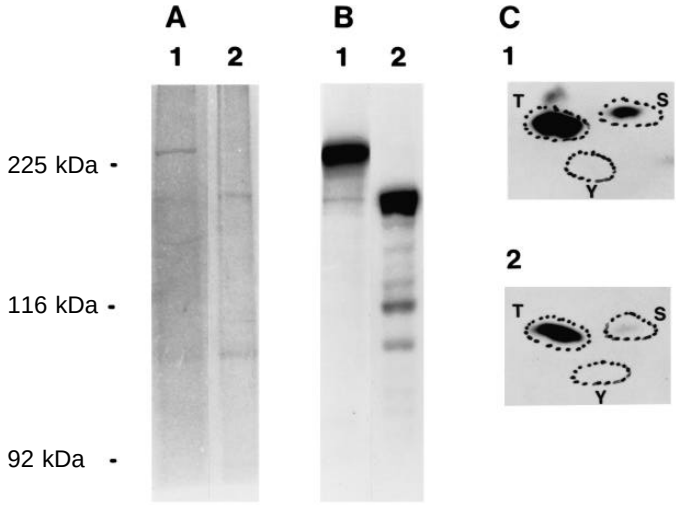

Fig. 10. Phosphorylation of wild-type and MyΔ934-1454 myosins in isolated Triton X-100-resistant cytoskeletons. Following phosphorylation of the myosin, it was immunoprecipated, subjected to SDS-PAGE and stained with Coomassie Blue. Autoradiography was performed on the Coomassie-stained gel. The myosin bands were excised and subjected ot phosphoamino acid analysis. (A) Coomassie-stained gel of the immunoprecipitate. (B) Autoradiogram of the Coomassie-stained gel in A. (C) Autoradiogram of wild-type and MyΔ934-1454 myosin TLC plate following electrophoresis at pH 1.9 (migration from bottom to top, relative to figure) and at pH 3.5 (migration from right to left). Positions of the cold internal phosphoamino acid standards are indicated by dotted lines: S, phosphoserine; T, phosphothreonine; Y, phosphotyrosine. Wild-type myosin is represented by the number 1. MyΔ934-1454 is represented by the number 2.

and T4 myosins, there was an appreciable amount of phosphorylation in lower molecular mass proteins that was not seen with wild-type or T1 myosins. This may be due to a decreased affinity of the myosin heavy chain kinase toward the truncated myosins, which permits nonspecific phosphorylation of non-myosin proteins.

To test the possibility that any modification of the tail might eliminate normal MHC phosphorylation, we analyzed phosphorylation of a previously reported myosin deletion construct (MyΔ934-1454) in which the central 'S2' portion of the myosin tail was removed (Kubalek et al., 1992). This deletion produces a myosin that is at least partly functional in vivo. When assayed in crude isolated cytoskeletons, MyΔ934-1454 displayed relatively normal levels of MHC phosphorylation on threonine (Fig. 10B), demonstrating that the severely reduced phosphorylation observed for T1 and T2 MHC is a property specific to deletions of the carboxyl-terminal region of MHC. MyΔ934-21454, however, displayed no detectable phosphorylation on serine (Fig. 10C), suggesting that the serine-specific phosporylation sites on MHC may lie within the region bound by residues 934-1454.

DISCUSSION

The results reported in this study define a 35 amino acid domain in the *Dictyostelium* myosin tail that is necessary for assembly of myosin filaments and for restoration of cellular function. Earlier in vivo studies demonstrated that the ΔC34 myosin retained the ability to rescue the myosin null cell phenotype, indicating the competence of ΔC34 myosins for filament assembly (Egelhoff et al., 1991). Those in vivo results are corroborated by the biochemical data reported in this study in which the salt-dependent solubility of ΔC34 myosin was shown to be similar to the wild-type myosin (Fig. 5). T1 myosin and T2 myosin retained both in vivo and in vitro properties of assembly, while T3 myosin and T4 myosin lacked the ability to assemble in vivo or in vitro. These results define a domain required for assembly, located between the carboxyl terminus of T3 myosin and the carboxyl terminus of ΔC34 myosin (Fig. 1). This 35 amino acid domain is bounded by residues 1784 and 1819. These results are supported by the finding that My4 is the only anti-*Dictyostelium* myosin antibody to inhibit filament formation (Peltz et al., 1985), and epitope mapping of My4 shows that it binds between the carboxyl terminus of T3 myosin and the carboxyl terminus of ΔC34 myosin (Fig. 3).

The 35 amino acid assembly domain defined in the present study supports and further refines the results of O'Halloran et al. (1990). In their study, a 34 kDa segment, N-LMM-34, bounded by amino acids 1533 and 1819, expressed in *E. coli* was necessary and sufficient for assembly into paracrystals. The 35 amino acid segment identified in the current study represents the carboxyl 12% of N-LMM-34. The fact that the N-LMM-34 fragment is much smaller than the tail of T3 myosin and is able to assemble argues against a critical length of myosin tail being responsible for the inability of T3 myosin to assemble. It should also be emphasized that the lower expression levels found in the T3 MHC and T4 MHC transformants cannot explain their inability to assemble and restore cellular function, since the expression level of ΔC34 myosin was even lower than that of T3 and T4 myosins, and yet ΔC34 myosin was able to assemble and restore cellular function (Egelhoff et al., 1991).

The tail segment of *Dictyostelium* myosin displays a repetitive 28 amino acid repeat, where each repeat contains a repetitious pattern of charged residues (Warrick and Spudich, 1987). This repetitive 28 residue pattern is characteristic of all conventional myosin tails, and the charge pattern is thought to be important in the assembly of filaments (McLachlin, 1984). It is noteworthy that the 35 amino acid segment (amino acid residues 1784-1819) that we have identified as essential for filament formation lies directly upstream from two of the threonine phosphorylation sites (1823 and 1833) that appear to be involved in regulation of filament assembly. Luck-Vielmetter et al. (1990) recently observed that the 23 amino acid segment just upstream from the 1823 and 1833 phosphorylation sites contains the highest concentration of basic residues in the myosin tail, and postulated that this charge cluster might have a critical role in filament assembly and that filament phosphorylation in this region might interfere with filament-filament interactions necessary for assembly. Our in vitro and in vivo results strongly support the hypothesis that this region has a critical role in driving filament formation, as removal of this segment of the tail in our T3 truncation appears to completely eliminate competence for filament formation. The 28 amino acid repeat spanning the 1823 and 1833 target sites and the immediately upstream repeat may have a critical role in seeding filament assembly.

Egelhoff et al. (1991) recently reported that the carboxyl-terminal domain of the *Dictyostelium* myosin tail, which contains the threonine phosphorylation sites, plays a critical role in myosin filament disassembly and relocalization. It was suggested that the inability to phosphorylate the carboxyl terminus of the myosin tail hindered myosin filament dissociation into monomers. To elucidate further the putative role of phosphorylation of threonine residues 1823, 1833 and 2029 in the regulation of assembly, and validate the contribution of threonine residues in myosin tail phosphorylation, a correlation of the assembly properties of the truncated myosins to the amount of phosphorylation of the truncated myosins was made. Only T1 and T2 myosin had any detectable amount of phosphorylation (Fig. 9). However, the amount of phosphorylation seen in T1 was only 2% of the amount of phosphorylation observed in the wild-type myosin. This was significantly lower than would have been predicted on the basis of the molar loss of only threonine residue 2029. Furthermore, T2 myosin, which is truncated by an additional 12.2 kDa compared to T1 myosin but still has threonine residues 1823 and 1833, had only trace amounts of phosphorylation (Fig. 9). These results support the previous findings of O'Halloran et al. (1990), in which a cloned portion of the *Dictyostelium* myosin tail, N-LMM-37, containing threonine residues 1823 and 1833 expressed in *E. coli* was not phosphorylated. However, a larger fragment, LMM-58, whose amino acid boundaries are 1533-2034, was phosphorylated. LMM-58 is not only larger but contains all three putative threonine phosphorylation sites. To assure that lack of phosphorylation was not due to the length of the myosin tail, MyΔ934-1454 was subjected to the phosphorylation assay. MyΔ934-1454 has similar phosphorylation levels to those of wild-type myosin (Fig. 10B). Phosphoamino acid analysis of MyΔ934-1454 and wild-type myosin confirmed that the phosphorylation was predominantly threonine phosphorylation (Fig. 10C). The lack of serine phosphorylation found in MyΔ934-1454 also suggests that serine sites of phosphorylation may lie in the 521 amino acid region deleted from MyΔ934-1454. The phosphorylation data show that the 15 kDa carboxyl-terminal portion of the myosin tail is absolutely essential for efficient phosphorylation, even of threonine residues that are 12 kDa upstream. This terminal 15 kDa tip of the myosin tail may be needed as a recognition site for the MHC kinase. Alternatively, it is possible that phosphorylation of threonine residue 2029 in this 15 kDa region is a prerequisite for the phosphorylation of the other two phosphorylation sites.

Phosphorylation of the myosin tail is clearly not essential in allowing myosin to initiate motile cellular functions. T2 and ΔC34 myosins both assemble and maintain the ability to support cytokinesis, development and capping of surface proteins, while demonstrating no significant phosphorylation. The capping experiments and the Triton-insoluble cytoskeleton assay suggest that the role of phosphorylation is to induce disassembly and relocalization of the myosin filaments. T2 myosin demonstrated similar characteristics to ΔC34 myosin (Egelhoff et al., 1991) in these respects. T2 myosin maintains the ability to cap surface proteins but has a temporal defect in dissociating from beneath capped surface proteins. T2 myosin also abnormally fractionates to the Triton-insoluble cytoskeleton, further demonstrating properties of over-assembly. Thus, phosphorylation of the *Dictyostelium* myosin tail is involved in the regulation of disassembly of the myosin filaments and relocalization of myosin, and is therefore important in the fine-tuned motile process in vivo, even though the cells manage to divide and develop (somewhat inefficiently) without phosphorylation capability.

We thank T. Q. Uyeda for his helpful criticism of this manuscript. R. J. Lee was supported by a National Institutes of Health Physician Scientist Award AR01829-04. T. T. Egelhoff was supported by a Stanford Tumor Biology Training grant, CA 09151. This work was supported by a National Institutes of Health grant (GM 46551) to J. A. Spudich.

REFERENCES

Atkinson, S. J. and Stewart, M. (1992). Molecular interactions in myosin assembly. Role of the 28-residue charge repeat in the rod. *J. Mol. Biol.* **226**, 7-13.

Berlot, C. H., Spudich, J. A. and Devreotes, P. N. (1985). Chemoattractant-elicited increase in myosin phosphorylation in *Dictyostelium*. *Cell* **43**, 307-314.

Berlot, C. H., Devreotes, P. N. and Spudich, J. A. (1987). Chemoattractant-elicited increases in *Dictyostelium* myosin phosphorylation are due to changes in myosin localization and increases in kinase activity. *J. Biol. Chem.* **263**, 3918-3926.

Boyle, W. J., Van Der Geer, P. and Hunter, T. (1991). Phosphopeptide mapping and phosphoamino acid analysis by two-dimensional separation on thin-layer cellulose plates. *Meth. Enzymol.* **201**, 110-149.

Clark, M. and Spudich, J. A. (1974). Biochemical and structural studies of actomyosin-like proteins from non-muscle cells. Isolation and characterization of myosin from amoebae of *Dictyostelium discoideum*. *J. Mol. Biol.* **86**, 209-222.

Cohen, S., Knecht, D., Lodish, H. and Loomis, W. (1986). DNA sequences required for expression of a *Dictyostelium* actin gene. *EMBO J.* **5**, 3361-3366.

Cooper, J. A., Sefton, B. M. and Hunter, T. (1983). Detection and quantification of phosphotyrosine in proteins. *Meth. Enzymol.* **99**, 387-402.

Coté, G. P. and McCrea, S. M. (1987). Selective removal of the carboxyl-terminal tail end of the *Dictyostelium* myosin II heavy chain by chymotrypsin. *J. Biol. Chem.* **262**, 13033-13038.

De Lozanne, A., Berlot, C. H., Leinwand, L. A. and Spudich, J. A. (1987). Expression in *Escherichia coli* of a functional *Dictyostelium* myosin tail fragment. *J. Cell Biol.* **105**, 2999-3005.

De Lozanne, A. and Spudich, J. A. (1987). Distruption of the *Dictyostelium* myosin heavy chain gene by homologous recombination. *Science* **236**, 1086-1091.

Dynes, J. L. and Firtel, R. A. (1989). Molecular complementation of a genetic marker in *Dictyostelium* using a genomic DNA library. *Science* **86**, 7966-7970.

Egelhoff, T. T., Brown, S. S., Manstein, D. J. and Spudich., J. A. (1989). Hygromycin resistance as a selectable marker in *Dictyostelium discoideum*. *Mol. Cell Biol.* **9**, 1965-1968.

Egelhoff, T., Manstein, D. and Spudich, J. (1990). Complementation of myosin null mutants in *Dictyostelium discoideum* by direct functional selection. *Dev. Biol.* **137**, 359-367.

Egelhoff, T. T., Brown, S. S. and Spudich, J. A (1991). Spatial and temporal control of nonmuscle myosin localization: Identification of a domain that is necessary for myosin filament disassembly in vivo. *J. Cell Biol.* **112**, 677-688.

Egelhoff, T. T., Lee, R. J. and Spudich, J. A. (1993). *Dictyostelium* myosin heavy chain phosphorylation sites regulate myosin filament assembly and localization in vivo. *Cell* **75**, 363-371.

Flicker, P., Peltz, G., Sheetz, M. D., Parham, P. and Spudich, J. A. (1985). Site-specific inhibition of myosin-mediated motility in vitro by monoclonal antibodies. *J. Cell Biol.* **100**, 1024-1030.

Fukui, Y., De Lozanne, A. and Spudich, J. (1990). Structure and function of the cytoskeleton of a *Dictyostelium* myosin-defective mutant. *J. Cell Biol.* **110**, 367-378.

Kelley, C. A, Kawamoto, S., Conti, M. A. and Adelstein, R. S. (1991). Phosphorylation of vertebrate smooth muscle and nonmuscle myosin heavy chains in vitro and in intact cells. *J. Cell Sci. Suppl. 14*, 49-54.

Knecht, D. and Loomis, W. (1987). Antisense RNA inactivation of myosin heavy chain gene expression in Dictyostelium discoideum. *Science* **236**, 1081-1086.

Kolega, J. and Taylor, D. L. (1993). Gradients in the concentration and assembly of myosin II in living fibroblasts during locomotion and fiber transport. *Mol. Biol. Cell* **4**, 819-836.

Kolodney, M. S and Elson, E. L. (1992). Correlation of myosin light chain phosphorylation with isometric contraction of fibroblasts. *J. Biol. Chem.* **268**, 23850-5.

Kubalek, E. W., Uyeda, T. Q. P. and Spudich, J. A. (1992). A *Dictyostelium* myosin II lacking a proximal 58-kDa portion of the tail is functional in vitro and in vivo. *Mol. Biol. Cell* **3**, 1455-1462.

Kuczmarski, E. R. and Spudich, J. A. (1980). Regulation of myosin self-assembly: phosphorylation of *Dictyostelium* heavy chain inhibits formation of thick filaments. *Proc. Nat. Acad. Sci. USA* **77**, 7292-7296.

Luck-Vielmetter, D., Schleicher, M., Grabatin, B., Wippler, J. and Gerisch, G. (1990). Replacement of threonine residues by serine and alanine in a phosphorylatable heavy chain fragment of *Dictyostelium* myosin II. *FEBS Lett.* **269**, 239-243.

Ludowyke R. I., Peleg I., Beaven M. A and Adelstein R. S. (1989). Antigen-induced secretion of histamine and the phosphorylation of myosin by protein kinase C in rat basophilic leukemia cells. *J. Biol. Chem*. **264**, 12492-501.

Manstein, D. J., Titus, M. A., De Lozanne, A. and Spudich, J. A. (1989). Gene replacement in *Dictyostelium*: generation of myosin null mutants. *EMBO J.* **8**, 923-932.

Marin, F. T. and Rothman, F. G. (1980). Regulation of development in *dictyostelium discoideum.* IV. effects of ions on the rate of differentiation and cellular response to cyclic AMP. *J. Cell Biol.* **87**, 823-0827.

McLachlin, A. D. (1984). Structural implications of the myosin amino acid sequence. *Annu. Rev. Bioeng.* **13**, 167-89.

O'Halloran, T. J., Ravid, S. and Spudich, J. A. (1990). Expression of *Dictyostelium* myosin in *Dictyostelium* myosin tail segments in *Escherichia coli*: domains required for assembly and phosphorylation. *J. Cell Biol.* **110**, 63-70.

Pagh, K., Maruta, H., Clavicz, M. and Garish, G. (1984). Localization of two phosphorylation sites adjacent to a region important for polymerization of the tail of *Dictyostelium* myosin. *EMBO J.* **3**, 3271-3278.

Pasternak, C., Spudich, J. A. and Elson, E. (1989). Capping of surface receptors and concomitant cortical tension are generated by conventional myosin. *Nature* **341**, 549-55.

Peltz, G., Spudich, J. A. and Parham, P. (1985). Monoclonal antibodies against seven sites on the head and tail of *Dictyostelium* myosin. *J. Cell Biol.* **100**, 1016-1023.

Ravid, S. and Spudich, J. A. (1989). Myosin heavy chain kinase from developed *Dictyostelium* cells: purification and characterization. *J. Biol. Chem.* **264**, 15144-15150.

Sagara, J., Nagata, K. and Ichikawa, Y. (1983). Phosphorylation of the myosin heavy chain. Its effects on actin-activated Mg^{2+}-stimulated ATPase in leukaemic myeloblasts. *Biochem. J.* **214**, 839-843.

Sambrook, J., Fritsch, E. F. and Maniatis, T. (1989). *Molecular Cloning: a Laboratory Manual.* Cold Spring Harbor Laboratory Press, Cold Spring Harbor, NY.

Sinard, J. H., Rimm, D. L. and Pollard, T. D. (1990). Identification of functional regions on the tail of Acanthamoeba myosin-II using recombinant fusion proteins. II. Assembly properties of tails with NH_2- and COOH-terminal deletions. *J. Cell Biol.* **111**, 2417-2426.

Somlyo, A. P. (1993). Myosin isoforms in smooth muscle: how may they affect function and structure? *J. Muscle Res. Cell Motil.* **14**, 557-563.

Sussman, M. (1987). Cultivation and synchronous morphogenesis of *Dictyostelium* under controlled experimental conditions. *Meth. Cell Biol*. **28**, 9-29.

Tan, J. L., Ravid, S. and Spudich, J. A. (1992). Contol of nonmuscle myosins by phosphorylation. *Annu. Rev. Biochem*. **61**, 721-729.

Trybus, K. M. (1991). Regulation of smooth muscle myosin. *Cell Motil. Cytoskel.* **18**, 81-5.

Vaillancourt, J., Lyons, C. and Coté, G. (1988). Identification of two phosphorylated threonines in the tail region of *Dictyostelium* myosin II. *J. Biol. Chem.* **263**, 10082-1087.

Warrick, H. M. and Spudich, J. A. (1987). Myosin structure and function in cell motility. *Annu. Rev. Cell. Biol.* **3**, 379-421.

Yumura, S., Murata, H. and Fukui, Y. (1984). Localization of actin and myosin for the study of ameboid movement in *Dictyostelium* using improved immunofluorescence. *J. Cell Biol.* **99**, 894-899.

(Received 7 April 1994 - Accepted 9 June 1994)